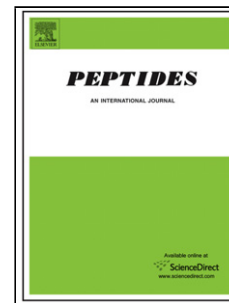


Accepted Manuscript

Title: Metabolism of Peptide YY 3–36 in Göttingen Mini-pig and Rhesus Monkey

Author: Jørgen Olsen Jacob Kofoed Søren Østergaard Birgitte S. Wulff Flemming S. Nielsen Rasmus Jorgensen



PII: S0196-9781(16)30010-9
DOI: <http://dx.doi.org/doi:10.1016/j.peptides.2016.01.010>
Reference: PEP 69592

To appear in: *Peptides*

Received date: 21-10-2015
Revised date: 4-1-2016
Accepted date: 11-1-2016

Please cite this article as: Olsen Jorgen, Kofoed Jacob, Ostergaard Soren, Wulff Birgitte S, Nielsen Flemming S, Jorgensen Rasmus. Metabolism of Peptide YY 3–36 in Göttingen Mini-pig and Rhesus Monkey. *Peptides* <http://dx.doi.org/10.1016/j.peptides.2016.01.010>

This is a PDF file of an unedited manuscript that has been accepted for publication. As a service to our customers we are providing this early version of the manuscript. The manuscript will undergo copyediting, typesetting, and review of the resulting proof before it is published in its final form. Please note that during the production process errors may be discovered which could affect the content, and all legal disclaimers that apply to the journal pertain.

Metabolism of Peptide YY 3-36 in Göttingen Mini-pig and Rhesus Monkey

Jørgen Olsen ^{a*}, Jacob Kofoed ^b, Søren Østergaard ^c, Birgitte S. Wulff ^d, Flemming S. Nielsen ^e and Rasmus Jorgensen ^f

^a Discovery ADME , Novo Nordisk A/S, Måløv, Denmark

^b Protein & Peptide Chemistry 3, Novo Nordisk A/S, Måløv, Denmark

^c Protein & Peptide Chemistry 2, Novo Nordisk A/S, Måløv, Denmark

^d Diabetes & Obesity Biology, Novo Nordisk A/S, Måløv, Denmark

^e Pharmacology 2, Novo Nordisk A/S, Måløv, Denmark

^f Histology & Diabetes Pharmacology Novo Nordisk A/S, Måløv, Denmark

Corresponding author:

Jørgen Olsen, PhD

Novo Nordisk A/S

Discovery ADME

Discovery Biology & Technology, Global Research

DK-2760 Måløv

Denmark

E-mail: jqgo@novonordisk.com

Highlights

- The major metabolite of PYY₃₋₃₆-amide in mini-pig and rhesus monkey was PYY₃₋₃₄.
- Metabolism of PYY₃₋₃₆-amide to PYY₃₋₃₄ may be a two-step process via PYY₃₋₃₅.
- C-terminal degradation of PYY₁₋₃₆-amide and PYY₃₋₃₆-amide was similar.

Abstract

Peptide YY 3-36-amide (PYY₃₋₃₆) is a peptide hormone, which is known to decrease appetite and food-intake by activation of the Y₂ receptor. The current studies were designed to identify the metabolites of PYY₃₋₃₆ in mini-pig and rhesus monkey. Plasma samples were analyzed by high resolution LC-MS (and MS/MS) in order to unambiguously identify the metabolites of PYY₃₋₃₆. In summary, the metabolism of PYY₃₋₃₆ was similar in mini-pig and rhesus monkey. Several metabolites were identified and PYY₃₋₃₄ was identified at the highest levels in plasma. In addition, mini-pigs were also dosed with PYY₁₋₃₆-amide, PYY₃₋₃₅, PYY₃₋₃₄ and [*N*-methyl 34Q]-PYY₃₋₃₆-amide in order to investigate the mechanisms by which PYY was metabolized. PYY₃₋₃₅ was rapidly converted to PYY₃₋₃₄ whereas dosing of PYY₃₋₃₄ to mini-pigs only showed circulating degradation products at low levels, i.e., PYY₃₋₃₄ was metabolically more stable than PYY₃₋₃₆ and PYY₃₋₃₅. [*N*-methyl 34Q]-PYY₃₋₃₆-amide was hypothesized to be stable towards cleavage between 34Q and 35R and after i.v. administration to mini-pigs, one major cleavage product was identified as [*N*-methyl 34Q]-PYY₃₋₃₅. Overall, this showed that cleavage between 35R and 36Y was possible as well as between 34Q and 35R (as shown for PYY₃₋₃₅), which indicated that metabolism of PYY₃₋₃₆ to PYY₃₋₃₄ may be a two-step process. PYY₁₋₃₆ was also dosed to mini-pigs, which showed that PYY₁₋₃₆ was metabolized in the C-terminal as PYY₃₋₃₆. The overall degradation pattern of PYY₁₋₃₆ was more complex due to the simultaneous enzymatic degradation in the N-terminal to form PYY_{2-34/36} and PYY_{3-34/36}. In

vitro incubations with heparin stabilized plasma showed that PYY₃₋₃₆ was degraded with a half-life of 175 min, whereas incubations with PYY₃₋₃₅ (half-life of 6 min) showed a rapid formation of PYY₃₋₃₄. In conclusion, the present studies showed that PYY₃₋₃₆ underwent enzymatic degradation in the C-terminal part and that the major circulating metabolite was PYY₃₋₃₄. Furthermore, it may be a sequential two-step process leading to the formation of PYY₃₋₃₅ and subsequently the metabolically more stable PYY₃₋₃₄.

Abbreviations:

AUC, Area under the curve; DPP-IV, Dipeptidyl peptidase 4; EIC, extracted ion chromatogram; LC-MS, Liquid chromatography mass spectrometry; m/z, mass-to-charge ratio; NPY, neuropeptide Y; ppm, parts per million; PYY₃₋₃₆, Peptide YY 3-36; PP, pancreatic polypeptide; z, charge; TFA, trifluoroacetic acid.

Keywords:

PYY₃₋₃₆

In Vivo Metabolism

Liquid Chromatography Mass Spectrometry (LC-MS)

1 Introduction

Peptide YY (PYY) is a 36 amino acid gut hormone [4], and a member of a family of closely related peptides including neuropeptide Y (NPY) and pancreatic polypeptide (PP), collectively named the NPY hormone family, which activate a group of receptors called Y receptors (Y₁, Y₂, Y₄ and Y₅) with different specificity.

PYY circulates in two active forms, PYY₁₋₃₆ and PYY₃₋₃₆, and whereas PYY₁₋₃₆ activates Y₁, Y₂ and Y₅ receptors, PYY₃₋₃₆ displays increased selectivity for the Y₂ receptor although some Y₁ and Y₅ affinity is retained [12]. Y₂ receptor activation is known to decrease appetite and food-intake whereas Y₁ and Y₅ receptor activation leads to an increase in appetite and food intake.

PYY₃₋₃₆ has been shown to reduce appetite and food intake in several species including humans [6]. This effect of PYY₃₋₃₆ on food intake and body weight was shown to be mediated through the Y₂ receptor as co-administration of a Y₂ selective antagonist attenuated the effect of PYY₃₋₃₆ on food intake in rodents [1]. Other physiological effects attributed to PYY include slowing of intestinal transit, inhibition of gastrointestinal anion and electrolyte secretion [7] and lowering of blood glucose [15, 17].

PYY₁₋₃₆ is degraded to PYY₃₋₃₆ by dipeptidyl peptidase IV (DPP-IV), which is ubiquitously distributed with high levels in e.g., kidney and bile, but DPP-IV is also present in a soluble form in plasma [8, 10, 14]. Moreover, PYY₁₋₃₆ has also been shown to be a substrate for the metalloprotease aminopeptidase P, which removes the N-terminal tyrosine from PYY₁₋₃₆ to form PYY₂₋₃₆ [13]. Besides degradation in the N-terminal, in vitro studies have also shown that PYY is cleaved by endopeptidase 24.11 at the 29N-30L bond [13]. In addition, incubation with kidney brush border preparations have identified cleavage sites between 10E-

11D, 12A-13S and 14P-15E of which the first two cleavage sites were similar to those observed after incubation with meprin β [3].

The in vivo metabolism of the C-terminal of PYY₃₋₃₆ has recently been investigated in pigs [18]. Plasma samples from this study were analyzed with a radioimmunoassay using an antiserum, which detected PYY_{1-34/3-34} and showed negligible cross-reaction with PYY_{1-36/3-36}. Important conclusions on the metabolism of PYY₃₋₃₆ could be drawn from the studies showing that C-terminal metabolites, most likely PYY₃₋₃₄, were formed during infusion of PYY₃₋₃₆ to pigs. Furthermore, it was demonstrated that C-terminal degradation took place in the liver and that both PYY₃₋₃₄ and PYY₃₋₃₆ were eliminated by the kidneys. Incubation studies with plasma and blood also showed C-terminal degradation of PYY₃₋₃₆ although the degradation rate appeared to be low compared to the rapid degradation observed in vivo.

NPY shares 70% sequence identity with PYY, which suggests that there could be similarities in the degradation of PYY and NPY. In human serum, NPY₁₋₃₆ is degraded rapidly by DPP-IV to NPY₃₋₃₆ and to a lesser extent by plasma kallikrein to NPY₃₋₃₅, and to NPY₂₋₃₆ by aminopeptidase P. Furthermore, NPY₁₋₃₂, NPY₁₋₃₄, NPY₁₋₃₅, NPY₂₋₃₂, NPY₂₋₃₄, NPY₂₋₃₅, NPY₃₋₃₂ and NPY₃₋₃₄ were detected at lower levels [2]. A similarly complex degradation pattern was observed for NPY-analogues labelled with carboxyfluorescein following incubation with serum, which e.g. led to cleavage between 32T-33R, 34Q-35R and 35R-36Y [11].

Apart from DPP-IV cleavage of PYY₁₋₃₆ [9] and the study on PYY₃₋₃₆ in pig by Toräng *et al.* [18], the degradation of PYY₁₋₃₆ and PYY₃₋₃₆ has predominantly been investigated in experiments with tissue preparations, recombinant enzymes or plasma/serum. The current

studies were designed to address the metabolism of PYY₃₋₃₆ in mini-pig and rhesus monkey and to further characterize the *in vivo* metabolic routes by which PYY₃₋₃₆ was degraded. Plasma analysis was conducted by LC-MS in order to unambiguously identify metabolites of PYY₃₋₃₆. This allowed a detailed characterization of the metabolites circulating in plasma without the risk of assay interference from e.g., cross-reactivity with related metabolites/peptides and without the need for antibodies raised against potential metabolites of interest. Insights into the metabolism of PYY₃₋₃₆ came from additional studies in mini-pig with PYY₃₋₃₅, PYY₃₋₃₄ and a stabilized analogue of PYY₃₋₃₆, [*N*-methyl 34Q]-PYY₃₋₃₆. The sequences of the studied peptides are summarized in Figure 1.

2 Materials and Methods

2.1 Chemicals

All chemicals were of analytical grade or higher. Ethanol (96% v/v), triisopropylsilane, *N,N'*-diisopropylcarbodiimide, and formic Acid ($\geq 98\%$) were from Sigma Aldrich, Chemie GmbH (Steinheim, Germany). Acetonitrile (LiChrosolve), trifluoroacetic acid (TFA), sodium dihydrogen phosphate, disodium hydrogen phosphate and sodium chloride were purchased from Merck KGaA (Darmstadt, Germany). Water came from a MilliQ equipment (Advantage A10) from Millipore (Molsheim, France). Aprotinin (Trasylol) was from Bayer Health Care AG (Leverkusen, Germany) and valine-pyrrolidide was produced in house. Rink-amide or PAL polystyrene resins were purchased from Novabiochem (Darmstadt, Germany). Standard Fmoc amino acids and coupling reagents, 1-hydroxybenzotriazole (HObt) and Oxyma Pure were from Novabiochem (Darmstadt, Germany) or Protein Technologies (Tucson, USA). Fmoc-MeGln(Trt)-OH was from Watanabe Chemical Industries (Hiroshima, Japan). *N*-methyl pyrrolidine and piperidine were from Biosolve (Dieuze, France). PYY₁₋₃₆ was from Sigma Aldrich, Chemie GmbH (Steinheim, Germany). Pooled heparin plasma from mini-pig was purchased from Bioreclamation, Inc. (Westbury, NY).

2.2 Peptide synthesis

PYY₃₋₃₆, PYY₃₋₃₅, PYY₃₋₃₄, and *N*-methyl-Q34-PYY₃₋₃₆ were prepared using a Prelude peptide synthesizer (Protein Technologies, Tucson, Arizona US) and employing an Fmoc-chemistry protocol (6-8 eq. AA, 8 eq. *N,N'*-diisopropylcarbodiimide and 8 eq. 1-hydroxybenzotriazole or 8 eq OxymaPure® and 25% piperidine in *N*-methyl pyrrolidine to remove the Fmoc-group). Coupling time was set to 80 min while coupling with Fmoc-Arg(Pbf)-OH was performed using double couplings and a total time of 2 hours. The peptides were cleaved and de-protected with TFA/triisopropylsilane/thioanisole (95:2.5:2.5) for 1-3 hours and precipitated with tert-butyl methyl ether or diethyl ether. After washing with tert-butyl methyl ether or diethyl ether through a 0.45 µm filter or centrifugation, the peptides were dried. The peptides were then purified by preparative HPLC using the following linear gradient: 15-40% acetonitrile with 0.1% trifluoroacetic acid over 40 min on a SymmetryPrep C18 19x300 mm, 7µm column (Waters Corporation, Milford, USA) eluting at 20 ml/min.

Molecular weights were determined using matrix-assisted laser desorption and ionization time-of-flight mass spectroscopy, recorded on a Microflex or Autoflex (Bruker Daltonics, Bremen, Germany). A matrix of alpha-cyano-4-hydroxy cinnamic acid was used.

PYY₃₋₃₆-amide

The title compound was synthesized on ChemMatrix Rink Amide resin (500 mg, 0.49 mmol/g,) and was obtained as a colorless foamy solid (31 mg, 3%, as TFA-salt). MALDI MS(+): Calculated for C₁₈₀ H₂₇₉ N₅₃ O₅₄: 4049.464, found: 4049.741.

PYY₃₋₃₅

The title compound was synthesized on Fmoc-Arg(Pbf)-Wang resin (500 mg, 0.60 mmol/g) and was obtained as a colorless foamy solid (45 mg, 4%, as TFA-salt). MALDI MS(+): Calculated for C₁₇₁ H₂₆₉ N₅₁ O₅₃: 3887.276, found: 3886.525.

PYY₃₋₃₄

The title compound was synthesized on Fmoc-Gln(Trt)-Wang resin (650 mg, 0.68 mmol/g) and was obtained as a colorless foamy solid (93 mg, 5%, as TFA-salt). MALDI MS(+): Calculated for C₁₆₅ H₂₅₇ N₄₇ O₅₂: 3731.090, found: 3730.020.

N-methyl-Q34-PYY₃₋₃₆-amide

The title compound was synthesized on TentaGel Rink amide resin (400 mg, 0.24 mmol/g) and was obtained as a colorless foamy solid (11 mg, 3%, as TFA-salt). MALDI MS(+): Calculated for C₁₈₁ H₂₈₁ N₅₃ O₅₄: 4061.081, found: 4061.498.

2.3 Mini-pig *in vivo* studies

The *in vivo* studies in mini-pigs were conducted at Novo Nordisk A/S with protocols approved by the Animal Experiments Inspectorate, Ministry of Justice, under the license number 2007/561–1276. A central venous catheter was implanted in animals (male Göttingen mini-pigs, 20–30 kg from Ellegaard Göttingen Minipigs A/S, Denmark) prior to commencement of studies [16]. Each mini-pig received the appropriate dose (30–50 nmol/kg) intravenously in a volume of 0.25 mL/kg (50 nmol/mL test compound in a vehicle containing 145 mM NaCl, 50 mM Na₂HPO₄, 0.05% Tween 80, pH 7.4 and filtered (0.42 µm)). Single administration of PYY₃₋₃₆ did not result in any clinical signs and was well tolerated in all animals. Blood samples were collected from all animals at pre-dose and at frequent intervals post-dosing in order to capture the exposure profile of the parent compound and metabolites

(e.g., 2, 4, 6, 8, 10, 12, 15, 20, 25, 30, 35, 45, 60, 75, 90, 105 and 120 min post-dosing). Blood samples were taken from the central venous catheter into test tubes containing buffer for stabilization (EDTA (disodium) 0.18 M, Aprotinin 15000 KIE/ml, valine-pyrrolidide 0.30 mM, pH adjusted 7.4) in a volume of buffer of 50 μ L per mL of blood. Aprotinin was added to inhibit plasma kallikrein/serine proteases and valine-pyrrolidide to inhibit DPP-IV. EDTA is a commonly used anticoagulant, which also inhibits metalloproteases. The blood samples (0.7 mL) were kept on ice for maximum 10 min before centrifugation (1200 x g, 4°C, 10 min). Plasma were immediately transferred to Micronic-tubes and stored at -20°C until analysis.

2.4 Rhesus monkey *in vivo* studies

The *in vivo* studies in Rhesus monkeys were conducted at BioTest s.r.o (Czech Republic) in compliance with the European convention for the protection of vertebrate animals used for experimental and other scientific purposes (ETS 123), the Act of the Czech National Assembly, Collection of laws No. 246/1992, inclusive of the amendments, on the Protection of animals against cruelty, and Public Notice of the Ministry of Agriculture of the Czech Republic, Collection of laws No. 207/2004 as amended, on keeping and exploitation of experimental animals. The study protocol was approved by the Institutional Animal Care and Use Committee (IACUC at BioTest) and the Committee for Animal Protection of the Ministry of Industry and Trade of the Czech Republic (8/2009) as well as the Novo Nordisk internal Ethical Review Council. The animals (2 males and 1 female Rhesus monkey (purpose bred, BioTest, weighing 3.5-5.0 kg) were fasted overnight and until 3h after the dosing. Water was provided *ad libitum*. Each monkey received the appropriate dose (50 nmol/kg) intravenously in a volume of 1 mL/kg (50 nmol/mL test item in a vehicle containing 145 mM NaCl, 50 mM Na₂HPO₄, 0.05% Tween 80, pH 7.4 and filtered (0.42 μ m)) in *v.saphena*. Single administration of PYY₃₋₃₆ did not result in any clinical signs and was well tolerated in

all animals. Blood samples were collected from all animals at: pre-dose, 5, 10, 15, 30 and 45 minutes post dose and subsequently 1, 2, 4, 8, 12, 24, 48, 72 and 96 hours post dose. Blood samples were taken from *v. saphena* of the leg, which was not used for administration. Blood samples were collected into test tubes containing buffer for stabilization (EDTA (disodium) 0.18 M, Aprotinin 15000 KIE/mL, valine-pyrrolidide 0.30 mM, pH adjusted 7.4) in a volume of buffer of 50 μ L per mL of blood. The blood samples (0.7 mL) were kept on ice for max. 10 min before centrifugation (1200 x g, 4°C, 10 min). Plasma was immediately transferred to Micronic-tubes and stored at -20 °C until analysis.

2.5 LC-MS analysis

Plasma samples were analyzed by LC-MS on an LTQ Orbitrap (XL) mass spectrometer (Thermo Scientific, Bremen) to which Accela HPLC pumps and an autosampler were connected (both from Thermo Scientific). The mass spectrometer was equipped with an electrospray interface, which was operated in positive ionization mode. Analysis was conducted in full scan mode from m/z 300 - 1800 and at a resolution of 30000 (FWHM). HPLC was performed on a Jupiter Proteo column (4 μ m) 90 Å (50 x 2.0 mm ID) from Phenomenex (Torrance, CA). Mobile phases consisted of A: 0.1% formic acid and B: 0.1% formic acid in acetonitrile. The composition of mobile phase was held constant at 3%B from 0-3 min. Then a gradient from 3%B to 40%B was used from 3-10 min. The column was washed with 100%B for 2 min and then equilibrated with 3%B prior to next injection. The flow rate was 0.3 mL/min.

Plasma samples from the in vivo experiments were pooled at given time points and 30 μ L plasma was precipitated with 60 μ L acetonitrile containing 1% formic acid and 60 μ L ethanol (with 1% formic acid) and after centrifugation, 5 μ L of supernatant was injected onto the

column. Metabolites were not quantified, but the calibration curve for PYY₃₋₃₆ in plasma was linear from 2-1000 nM and parent PYY₃₋₃₆ was within this range. Two or three plasma standards were analyzed before and after the pooled samples in order to confirm stability of the LC-MS system. Furthermore, LC-MS responses (peak area) for calibration standards of PYY₃₋₃₆, PYY₃₋₃₅, PYY₃₋₃₄ and PYY₁₋₃₆ were shown to be similar, and therefore MS response was used as an estimate for levels of circulating metabolites compared to parent peptide.

2.6 *Identification of metabolites*

Metabolites were identified by high resolution MS and the major metabolites further characterized by MS/MS experiments. Raw data were examined with the program Pinpoint (version 1.2, ThermoScientific) for metabolite identification. To support the metabolite findings, MS spectra from LC-MS analysis were also inspected manually and the accurate mass measurements of potential metabolites were aligned with the sequence with the use of GPMW (version 8.21, Lighthouse Data). Extracted ion chromatograms of each metabolite were constructed by adding the most intense isotope peaks (mass window +/- 5 parts per million (ppm)) of the most abundant charge state. The LC-MS response (peak area) was plotted for each metabolite at the time points at which plasma samples were taken. The area under the curve (AUC) was calculated from the time profiles of each metabolite (from 2 min to last time point of exposure) and the AUC_{metabolite} relative to the AUC_{parent} was used as an estimate for the metabolite levels.

2.7 *In vitro metabolism studies with plasma*

A pool of heparin stabilized plasma from three mini-pigs was used for plasma stability studies of PYY₃₋₃₆ and PYY₃₋₃₅. One volume of 200 mM phosphate buffer (pH 7.4) was added to four volumes of plasma and the final concentration of PYY₃₋₃₆ (or PYY₃₋₃₅) was 1 μ M. Incubations

with plasma (n=4) were conducted at 37°C and aliquots were taken at 2, 5, 15, 30, 60, 120 and 240 min. A parallel study was conducted (n=4) in which 10 mM of EDTA was added to plasma. Incubations were stopped by addition of three volumes of cold ethanol and after centrifugation, the resultant supernatant was analyzed by LC-MS. Calibration standards of PYY₃₋₃₆ and PYY₃₋₃₅ were prepared in heparin plasma to which the inhibitor solution described under animal experiments was added. The analytical range in heparin-plasma was from 20-2000 nM and the calibration curve was fitted with a linear regression curve ($1/X^2$).

3 Results

3.1 Metabolism of PYY₃₋₃₆ in Mini-pig

The metabolism of PYY₃₋₃₆ in mini-pig was studied by LC-MS in two separate studies with two and four mini-pigs, respectively. The same metabolites were identified in both studies and based on MS response, PYY₃₋₃₄ was detected as the major metabolite of PYY₃₋₃₆ in both studies. An example of analysis is illustrated in Figure 2, which shows the extracted ion chromatograms (EIC) of PYY₃₋₃₆ and three metabolites, PYY₃₋₃₅, PYY₃₋₃₄ and PYY₃₋₃₀, in a plasma sample taken 20 min after dosing.

An MS spectrum from a time interval in which PYY₃₋₃₆ and most metabolites eluted (~7.9-8.2 min) is shown in Figure 3a. In the MS spectrum, the presence of PYY₃₋₃₆ and PYY₃₋₃₄ is shown at different charge states and in addition, PYY₃₋₃₀ was also detected at low levels. The most intense ion of PYY₃₋₃₄ was the $[M + 5H]^{5+}$ ion with a monoisotopic mass of m/z 746.7841. In addition, PYY₃₋₃₄ was observed with monoisotopic masses of m/z 622.4879 (z=6) and 933.2284 (z=4). All m/z values were in accordance with the proposed sequence of PYY₃₋₃₄ determined with a mass accuracy below 2 ppm. An MS/MS spectrum of PYY₃₋₃₄ (m/z 746.8, z=5) is illustrated in Figure 3b showing a series of y-ions of which the most dominant was the y_{30}^{4+} -ion, which represents cleavage between 4K and 5P. The monoisotopic mass of this fragment was m/z 872.9336 (2 ppm mass accuracy) and the most intense isotope

was m/z 873.1840. In addition, mainly triple charged y-ions were observed and all monoisotopic masses were in accordance with the proposed sequence of PYY₃₋₃₄, determined with mass accuracies below 5 ppm.

Further confirmation of the identity of PYY₃₋₃₄ came from experiments with the reference standard of PYY₃₋₃₄ spiked to plasma, which showed the same retention time, charge distribution and MS/MS spectrum as observed in plasma samples from mini-pigs dosed with PYY₃₋₃₆ (see supplementary data, Figure S1). Similarly, the reference standard of PYY₃₋₃₅ became available and this standard also had the same retention time and the same ion distribution as that observed in plasma samples from mini-pig. Other metabolites represented predominantly cleavage in the C-terminal resulting in formation of PYY₃₋₃₃, PYY₃₋₃₂, PYY₃₋₃₀, PYY_{3-29/4-30} and PYY₆₋₃₆. It was not possible to distinguish PYY₃₋₂₉ from PYY₄₋₃₀ by LC-MS since these two degradation products had the same monoisotopic mass. A summary of all the identified metabolites in mini-pig of PYY₃₋₃₆ is shown in Table 1.

The time profiles of parent/metabolites based on MS response are shown in Figure 4 from which it is seen that PYY₃₋₃₄ was the metabolite that circulated at the highest levels. This was further emphasized from LC-MS analysis of plasma standards containing PYY₃₋₃₆, PYY₃₋₃₅, PYY₃₋₃₄ and PYY₁₋₃₆, which showed that the MS response factors were similar. The response factors relative to the $[M + 6H]^{6+}$ -ion of PYY₃₋₃₆, when spiked to plasma (200 nM), were: 100% for PYY₁₋₃₆ ($z=6$ -ion), 73% for PYY₃₋₃₅ ($z=6$ -ion) and 94% for PYY₃₋₃₄ ($z=5$ -ion). These data can be found in supplementary data (Figure S1). The levels for the more truncated peptide metabolites, e.g., PYY₃₋₂₉, were more difficult to assess due to the lack of authentic standards. Nevertheless, they all appeared to be circulating at lower levels.

3.2 Metabolism of PYY₃₋₃₆ in Rhesus Monkey

Three rhesus monkeys were dosed with PYY₃₋₃₆ and the results from the study are summarized in Table 1. The metabolism took place in the C-terminal part of the peptide and was similar to the metabolites identified in mini-pig. PYY₃₋₃₄ was detected at the highest levels and at lower levels, PYY₃₋₃₅, PYY₃₋₃₃, PYY₃₋₃₀, PYY_{3-27/4-28}, PYY₃₋₂₆ and PYY₆₋₃₆ were observed. The reference standards of PYY₃₋₃₅ and PYY₃₋₃₄ co-eluted chromatographically and had the same monoisotopic masses, isotope pattern and charge state distribution as the metabolites observed in plasma samples from monkeys. In Table 1, the MS data are from analysis of samples from mini-pig. The corresponding MS data (monoisotopic masses) from rhesus monkey were all determined with a mass accuracy of 3 ppm (see supplementary data, Table S1).

3.3 Metabolism of PYY₍₁₋₃₆₎ in Mini-pig

The metabolism in the C-terminal was further addressed in a study with PYY₁₋₃₆, which compared to PYY₃₋₃₆ has a tyrosine and proline residue in position 1 and 2, respectively. The metabolism in the C-terminal part of the peptide was consistent with that described for PYY₃₋₃₆, i.e., loss of 35R and 36Y, and in addition metabolites originating from degradation of the N-terminal as a result of cleavage between 1Y-2P and 2P-3I. At later time points (> 60 min), PYY₃₋₃₄ was the predominant metabolite detected. Experiments with reference standards of PYY₃₋₃₆ and PYY₃₋₃₄ spiked to plasma confirmed the identification of these two PYY₁₋₃₆ metabolites. The identified metabolites are summarized in Table 2 showing that, based on MS response, PYY₃₋₃₆ was the major metabolite. The time profile can be found in supplementary data (Figure S2).

3.4 Metabolism of PYY₃₋₃₅, PYY₃₋₃₄ and [N-methyl 34Q]-PYY₃₋₃₆ in Mini-pig

To explore the mechanisms underlying metabolism of PYY₃₋₃₆ to PYY₃₋₃₄, three additional *in vivo* studies were conducted. The metabolism of PYY₃₋₃₅ and PYY₃₋₃₄ was evaluated in mini-pigs and in addition, an analogue, [N-methyl 34Q]-PYY₃₋₃₆, was also evaluated to investigate the effect on metabolism.

In the mini-pig study with PYY₃₋₃₅, PYY₃₋₃₄ was identified as the major metabolite of PYY₃₋₃₅. PYY₃₋₃₄ was detected at much higher levels than PYY₃₋₃₅ at all the time points from 2-120 min showing that PYY₃₋₃₅ was rapidly converted into PYY₃₋₃₄ in mini-pig. PYY₃₋₃₀, PYY_{3-29/4-30}, PYY_{3-27/4-28} and PYY₃₋₂₆ were also identified, and here the levels resembled what was observed when PYY₃₋₃₆ was dosed to mini-pig. The time profiles based on MS responses are shown in Figure 5 and MS data for each metabolite is shown in Table 3.

The metabolism of PYY₃₋₃₄, which was the major metabolite of PYY₃₋₃₆ and PYY₃₋₃₅, was also studied in mini-pigs. PYY₃₋₃₀, PYY_{3-29/4-30}, PYY_{3-27/4-28}, PYY₃₋₂₆ and PYY₆₋₃₄ were identified as shown in Table 4. Based on MS responses, the levels of these metabolites were low, which was accordance with the results from mini-pig studies with PYY₃₋₃₆ and PYY₃₋₃₅. Thus, the data showed that PYY₃₋₃₄ was metabolically more stable than PYY₃₋₃₆ or PYY₃₋₃₅.

This led to a study in mini-pig of [N-methyl Q34]-PYY₃₋₃₆, which was hypothesized to be stable towards proteolytic cleavage between 34Q and 35R. The study in mini-pig showed that the cleavage between 34Q and 35R was blocked and the metabolite observed at the highest levels was [N-methyl 34Q]-PYY₃₋₃₅ and at much lower levels, PYY₃₋₃₀, PYY_{3-27/4-28} and [N-methyl Q34]-PYY₆₋₃₆ were observed. All metabolites identified in mini-pig are summarized in Table 5. Identification of the major metabolite of [N-methyl 34Q]-PYY₃₋₃₅ is shown in Figure 6, which is an MS spectrum from a time interval, in which both [N-methyl 34Q]-PYY₃₋₃₅ and

[*N*-methyl 34Q]-PYY₃₋₃₆ eluted. Based on the MS signal intensity, the metabolite circulated at relatively high levels compared to the other identified metabolites of [*N*-methyl 34Q]-PYY₃₋₃₆.

3.5 *In vitro* plasma stability studies

Plasma stability studies with heparin-plasma from mini-pig showed that PYY₃₋₃₆ was degraded with a mean first order half-life of 175 min (n=4) (Data are shown in supplementary data, Figure S3). The mean rate constant from the experiments was $0.00397 \text{ min}^{-1} \pm 0.000259 \text{ min}^{-1}$ (n=4). Many metabolites were formed over time and therefore, metabolites with an MS response below 10% of parent PYY₃₋₃₆ are not discussed further. PYY₃₋₃₄ and PYY₃₋₃₂ were identified as the main metabolites formed over time and in addition, PYY₃₋₃₅ and PYY₃₋₃₃ were detected at lower levels. In an incubation study conducted in parallel, the effect of 10 mM EDTA on plasma stability was evaluated. Here, the half-life was measured to be 220 min (mean rate constant was $0.00315 \text{ min}^{-1} \pm 0.000159 \text{ min}^{-1}$, n=4). The presence of EDTA increased PYY₃₋₃₅ levels and inhibited formation of PYY₃₋₃₄ and furthermore, the presence of EDTA increased levels of PYY₃₋₃₃. A similar study was conducted for PYY₃₋₃₅, which had a mean first order half-life of 6 min (mean rate constant was 0.115 ± 0.00503 , n=4), whereas the half-life was 39 min (mean rate constant was 0.0179 ± 0.00225 , n=4) in the presence of 10 mM EDTA. MS data showed that PYY₃₋₃₅ was rapidly metabolized to PYY₃₋₃₄, which was identified as the major metabolite. For instance, PYY₃₋₃₄ levels were about 5-6-fold higher than PYY₃₋₃₅ after 15 min of incubation and were constant for the remaining part of the experiment (See supplementary data, Figure S3).

4 Discussion

The current studies were designed to identify the metabolites of PYY₃₋₃₆ *in vivo* and to further investigate the metabolic routes by which PYY₃₋₃₆ was metabolized. The doses were selected to give an initial plasma concentration of about 500 nM of PYY₃₋₃₆, which was in accordance

with the sensitivity of the LC-MS method that was used in the studies, and which allowed an unambiguous identification of PYY₃₋₃₆ metabolites.

Several metabolites of PYY₃₋₃₆ were identified of which PYY₃₋₃₄ was found circulating in plasma at the highest levels in both mini-pig and Rhesus monkey. Although PYY₃₋₃₅ was only detected at low levels following administration of PYY₃₋₃₆, the studies suggest that the formation of PYY₃₋₃₄ may be a two-step mechanism via the relatively unstable PYY₃₋₃₅. As shown in Figure 5, in vivo administration of PYY₃₋₃₅ to mini-pig showed that PYY₃₋₃₅ was rapidly converted into PYY₃₋₃₄ and the remaining degradation products were similar to those observed when PYY₃₋₃₆ was dosed, i.e., low levels of metabolites such as e.g., PYY₃₋₃₀ and PYY₆₋₃₆. This was in good agreement with in vitro stability studies on PYY₃₋₃₅ incubated with heparin plasma, which showed a short half-life of PYY₃₋₃₅ and a simultaneous rapid formation of PYY₃₋₃₄ (See supplementary data, Figure S3).

PYY₁₋₃₆ was also metabolized in the C-terminal with a major cleavage site between 34Q and 35R, but the overall enzymatic degradation of PYY₁₋₃₆ was more complex as a consequence of the simultaneous N-terminal degradation to form PYY₂₋₃₆ and PYY₃₋₃₆ (and PYY₃₋₃₄). Formation of PYY₂₋₃₆ is consistent with metabolism by aminopeptidase P [13] whereas formation of PYY₃₋₃₆/PYY₃₋₃₄ was due to metabolism by DPP-IV.

The next step was to evaluate the metabolism of PYY₃₋₃₄ when dosed to mini-pigs, and here no major metabolites were identified. In contrast, the identified minor metabolites were in accordance with the minor degradation products observed for PYY₃₋₃₆ and PYY₃₋₃₅. Thus, the data showed that PYY₃₋₃₄ was metabolically more stable than PYY₃₋₃₆ and PYY₃₋₃₅ and consequently, this degradation product was detected as the major metabolite of PYY₃₋₃₆.

To investigate the mechanism(s) of the metabolism of PYY₃₋₃₆ further, a PYY₃₋₃₆ analogue containing an *N*-methyl Gln in position 34 ([*N*-methyl 34Q]-PYY₃₋₃₆) was studied in mini-pig. The results from this study showed that [*N*-methyl Q34]-PYY₃₋₃₆ was predominantly metabolized to the corresponding PYY₃₋₃₅ metabolite and that PYY₃₋₃₄ formation was blocked. This means that cleavage between 35R and 36Y was possible, and since PYY₃₋₃₅ was shown to be rapidly degraded to PYY₃₋₃₄, this supports the hypothesis that the metabolism of PYY₃₋₃₆ to PYY₃₋₃₄ may be a two-step mechanism via PYY₃₋₃₅. However, our data cannot rule out a contribution from a protease that cleaves PYY₃₋₃₆ to form PYY₃₋₃₄. This would either require dosing of a PYY analogue, which was stable towards proteolytic cleavage between 35R and 36Y or alternatively, experiments with specific enzyme inhibitors in order to rule out parallel pathways that produce PYY₃₋₃₄ directly.

The data presented in this publication are in good agreement with a recent study by Toräng *et al.* [18] who concluded that PYY₃₋₃₆ was rapidly metabolized to PYY₃₋₃₄ in pig. The study by Toräng *et al.* was designed as an infusion study and the plasma concentration of PYY₃₋₃₆ was closer to physiological levels than in the present studies. Concentration may theoretically impact the degradation pattern, but despite the differences in dose, PYY₃₋₃₄ was identified as the major metabolite in our studies in minipig/monkey and in pig by Toräng *et al.* [18]. Interestingly, an unidentified metabolite was observed by Toräng *et al.* [18], which based upon our observations, might be PYY₃₋₃₀, although the presence of PYY₃₋₃₅, or PYY_{3-29/4-30} cannot be ruled out as potential candidates.

Initial *in vitro* stability experiments with PYY₃₋₃₆ in EDTA plasma failed to predict the presence of the major metabolite PYY₃₋₃₄. The absence of cleavage in the C-terminal has also

been reported in other studies [2], e.g., studies with NPY in EDTA-stabilized plasma. In contrast, our studies with heparin stabilized plasma were more predictive with respect to the metabolites observed in vivo. Here, PYY₃₋₃₆ was degraded into mainly PYY₃₋₃₄ and PYY₃₋₃₂ where the latter metabolite was only observed at very low levels in vivo in mini-pig and not detected in monkey. This challenges the correlation between enzymatic stability of PYY₃₋₃₆ in plasma and in vivo formation of metabolites or simply suggests that other tissues/organs are involved in the metabolism of PYY₃₋₃₆ as also reported elsewhere [18]. In addition, the metabolism was relatively slow (half-life ~ 175 min) in plasma incubations compared to the in vivo metabolism, which also suggests that plasma is not the most important compartment for PYY₃₋₃₆ metabolism. In contrast, the metabolism of PYY₃₋₃₅ was rapid both in vivo and in vitro in plasma (half-life at 6.5 min) and one major metabolite was formed, which was PYY₃₋₃₄. The in vitro formation rate of PYY₃₋₃₄ was reduced when EDTA was added to plasma. Therefore, it seems plausible to suggest that a metallo-enzyme was involved and that this enzyme might be e.g., carboxypeptidase U/plasma carboxypeptidase B, which is a zinc containing protein that is inhibited by the addition of EDTA [5].

In conclusion, the present data in mini-pig and monkey show that PYY₃₋₃₆ underwent enzymatic degradation in the C-terminal part and that the main circulating metabolite was PYY₃₋₃₄. The studies furthermore show that the metabolism of PYY₃₋₃₆ is complex and data based analytical techniques that do not specifically measure PYY₃₋₃₆ or any of its metabolites should be interpreted with some caution. Additional mechanistic studies indicated that PYY₃₋₃₆ may be formed by a two-step mechanism via the short-lived intermediate, PYY₃₋₃₅.

Contributions

All authors contributed to research design and discussion of data and contributed to the writing of the manuscript. JO, JK, SØ and FSN conducted the experimental work.

Acknowledgement

Dr. Luise Gram Schleiss and Dr. Berit Ø. Christoffersen (Pharmacology 2, Novo Nordisk A/S, Måløv, Denmark) are acknowledged for their contributions to studies with mini-pigs.

References

- [1] Abbott CR, Small CJ, Kennedy A, Neary N, Sajedi A, Ghatei MA, et al. Blockade of the neuropeptide YY2 receptor with the specific antagonist BIIIE0246 attenuates the effect of endogenous and exogenous peptide YY(3-36) on food intake. *Brain Research*. 2005;1043:139-44.
- [2] Abid K, Rochat B, Lassahn P-G, Stöcklin R, Michalet S, Brakch N, et al. Kinetic Study of Neuropeptide Y (NPY) Proteolysis in Blood and Identification of NPY3–35: A NEW PEPTIDE GENERATED BY PLASMA KALLIKREIN. *Journal of Biological Chemistry*. 2009;284:24715-24.
- [3] Addison ML, Minnion JS, Shillito JC, Suzuki K, Tan TM, Field BCT, et al. A role for metalloendopeptidases in the breakdown of the gut hormone, PYY 3-36. *Endocrinology*. 2011;152:4630.
- [4] Adrian TE, Ferri GL, Bacarese-Hamilton AJ, Fuessl HS, Polak JM, Bloom SR. Human distribution and release of a putative new gut hormone, peptide YY. *Gastroenterology*. 1985;89:1070-7.
- [5] Barrett A, Rawlings ND, Woessner JF. *Handbook of Proteolytic Enzymes*. Second Edition ed: Elsevier Academic Press; 2004.
- [6] Batterham R, Cowley MA, Small CJ, Herzog H, Cohen MA, Dakin C, et al. Gut hormone PYY3-36 physiologically inhibits food intake. *Nature*. 2002;418:650-4.
- [7] Cox HM. Neuropeptide Y receptors antisecretory control of intestinal epithelial function. *Autonomic Neuroscience-Basic & Clinical*. 2007;133:76-85.
- [8] De Meester I, Vanhoof G, Lambeir A-M, Scharpé S. Use of immobilized adenosine deaminase (EC 3.5.4.4) for the rapid purification of native human CD26/dipeptidyl peptidase IV (EC 3.4.14.5). *Journal Of Immunological Methods*. 1996;189:99-105.
- [9] Grandt D, Schimiczek M, Beglinger C, Layer P, Goebell H, Eysselein VE, et al. Two molecular forms of Peptide YY (PYY) are abundant in human blood: characterization of a radioimmunoassay recognizing PYY 1–36 and PYY 3–36. *Regulatory Peptides*. 1994;51:151-9.
- [10] Keane FM, Yao T-W, Seelk S, Gall MG, Chowdhury S, Poplawski SE, et al. Quantitation of fibroblast activation protein (FAP)-specific protease activity in mouse, baboon and human fluids and organs. *FEBS Open Bio*. 2014;4:43-54.
- [11] Khan IU, Reppich R, Beck-Sickinger AG. Identification of neuropeptide Y cleavage products in human blood to improve metabolic stability. *Peptide Science*. 2007;88:182-9.
- [12] Levens NR FM, Galizzi J-P, Fauchere J-L, Della-Zuana, O, Lonchamp M. *Neuropeptide Y and Related Peptides*: Springer-Verlag; 2004.
- [13] Medeiros MD, Turner A. Processing and metabolism of Peptide-YY: Pivotal roles of dipeptidylpeptidase-IV, aminopeptidase-P, and endopeptidase-24.11. *Endocrinology*. 1994;134:2088-94.
- [14] Mentlein R. Dipeptidyl-peptidase IV (CD26)-role in the inactivation of regulatory peptides. *Regul Pept*. 1999;85:9-24.
- [15] Ortiz AA, Milardo L, Decarr L, Buckholz TM, Mays M, Claus T, et al. A novel long-acting selective neuropeptide y2 receptor polyethylene glycol-conjugated peptide agonist reduces food intake and body weight and improves glucose metabolism in rodents. *Journal Of Pharmacology And Experimental Therapeutics*. 2007;323:692-700.
- [16] Petersen SB, Nielsen FS, Ribel U, Sturis J, Skyggebjerg O. Comparison of the pharmacokinetics of three concentrations of insulin aspart during continuous subcutaneous insulin infusion (CSII) in a pig model. *Journal of Pharmacy and Pharmacology*. 2013;65:230-5.
- [17] Pittner RA, Moore CX, Bhavsar SP, Gedulin BR, Smith PA, Jodka CM, et al. Effects of PYY[3-36] in rodent models of diabetes and obesity. *International Journal of Obesity*. 2004;28:963-71.
- [18] Toräng S, Veedfald S, Rosenkilde MM, Hartmann B, Holst JJ. The anorexic hormone Peptide YY3–36 is rapidly metabolized to inactive Peptide YY3–34 in vivo. *Physiological Reports*. 2015;3:n/a-n/a.

	1	3	10	20	30	34	36																													
PYY ₁₋₃₆ -NH ₂	Y	P	I	K	P	E	A	P	G	E	D	A	S	P	E	E	L	N	R	Y	Y	A	S	L	R	H	Y	L	N	L	V	T	R	Q	R	Y
PYY ₃₋₃₆ -NH ₂			I	K	P	E	A	P	G	E	D	A	S	P	E	E	L	N	R	Y	Y	A	S	L	R	H	Y	L	N	L	V	T	R	Q	R	Y
PYY ₃₋₃₅ -COOH			I	K	P	E	A	P	G	E	D	A	S	P	E	E	L	N	R	Y	Y	A	S	L	R	H	Y	L	N	L	V	T	R	Q	R	
PYY ₃₋₃₄ -COOH			I	K	P	E	A	P	G	E	D	A	S	P	E	E	L	N	R	Y	Y	A	S	L	R	H	Y	L	N	L	V	T	R	Q		
[<i>N</i> -methyl Q34]-PYY ₃₋₃₆ -NH ₂			I	K	P	E	A	P	G	E	D	A	S	P	E	E	L	N	R	Y	Y	A	S	L	R	H	Y	L	N	L	V	T	R	Q	R	Y

Figure 1 Peptide sequences of the compounds evaluated in vivo. 34Q: *N*-methyl-34Q.

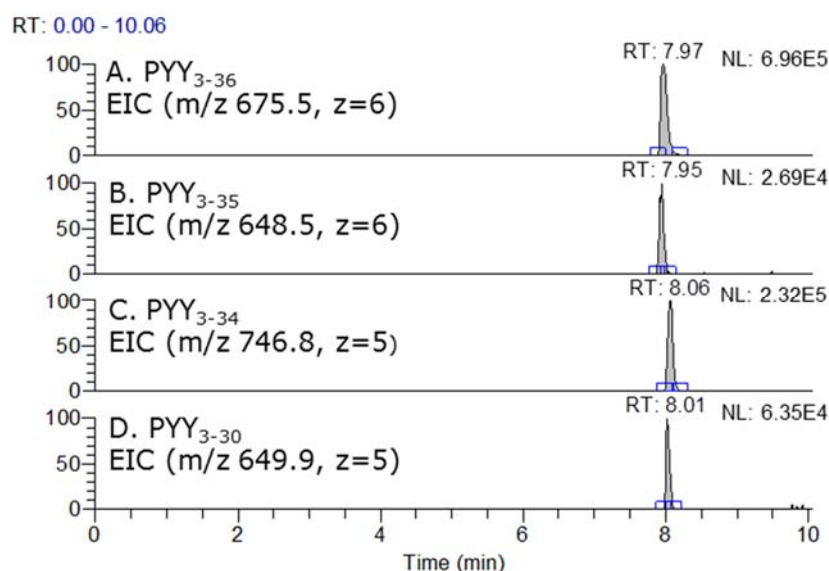


Figure 2 Extracted ion chromatograms (EICs) from LC-MS analysis of PYY₃₋₃₆ and three metabolites in mini-pig. The analyzed plasma sample was a pool of four samples taken 20 min after dose administration of PYY₃₋₃₆ (i.v., 50 nmol/kg). The extracted ion chromatograms were constructed by addition of the five most intense isotope peaks (± 5 ppm) for the most abundant charge state.

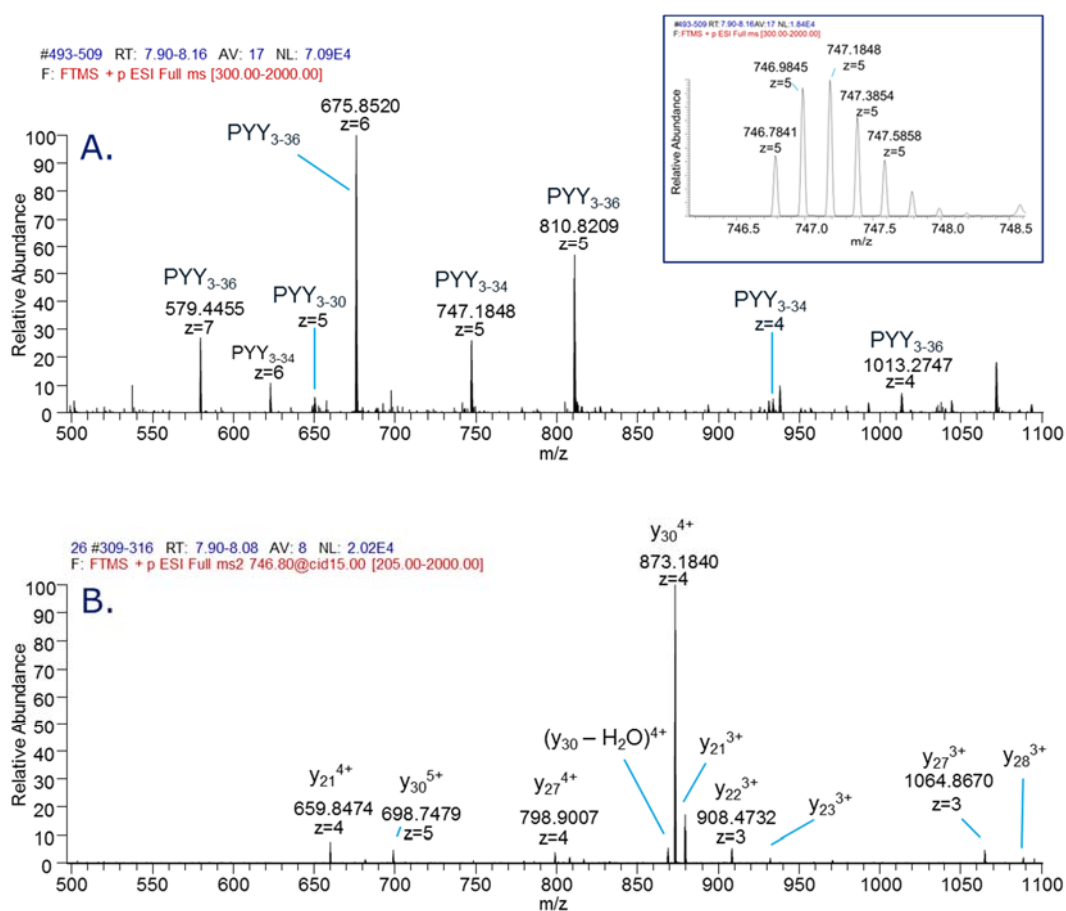


Figure 3 Identification of PYY₃₋₃₄ in a plasma sample taken 20 min after dose administration (50 nmol/kg, n=4) from mini-pigs dosed with PYY₃₋₃₆. A) Full scan spectrum from LC-MS analysis showing the presence of PYY₃₋₃₆ and PYY₃₋₃₄. A zoom from the full scan spectrum of the z=5 ion of PYY₃₋₃₄ is also shown. B) MS/MS spectrum of PYY₃₋₃₄ following LC-MS/MS analysis (m/z 746.8). All fragment ions were assigned with a mass accuracy below 5 ppm.

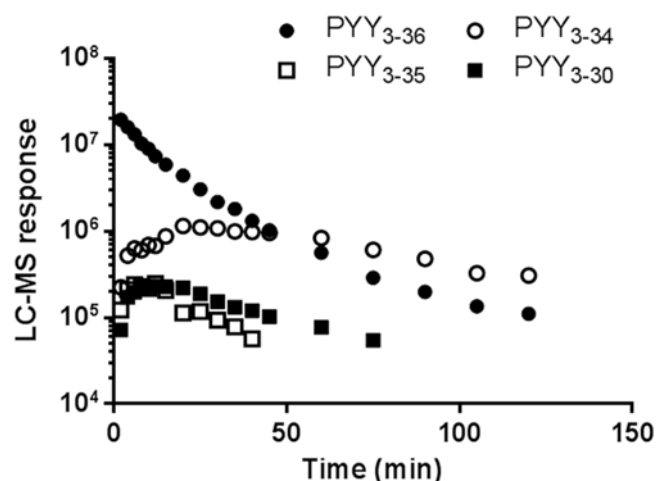


Figure 4 Time profiles of PYY₃₋₃₆ and the three most abundant metabolites after dose administration of PYY₃₋₃₆ to mini-pigs (i.v., 50 nmol/kg, n=4). Each time point represented LC-MS analysis of pooled samples (n=4). The LC-MS response of metabolites came from peak integration of extracted ion chromatograms.

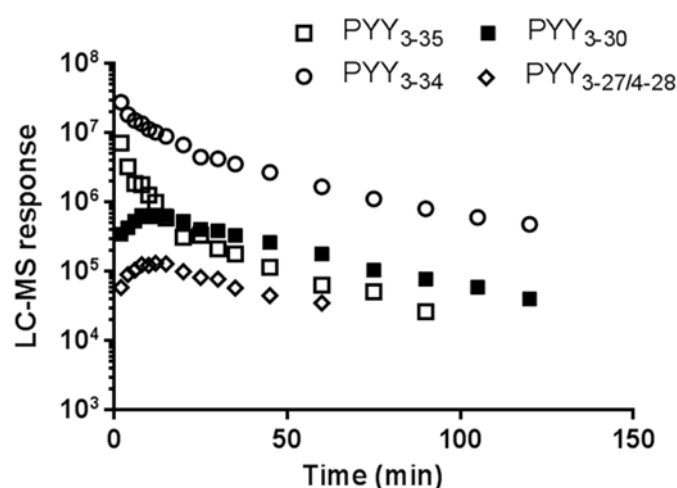


Figure 5 Time profiles of PYY₃₋₃₅ and the three most abundant metabolites after dose administration of PYY₃₋₃₅ (i.v., 50 nmol/kg) to a mini-pig. The LC-MS response of the metabolites came from peak integration of extracted ion chromatograms.

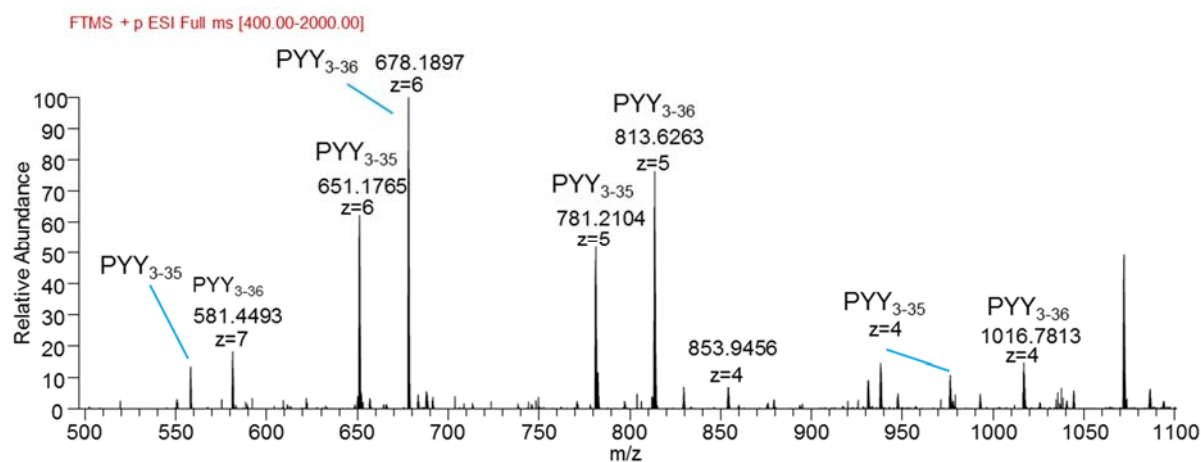


Figure 6 Identification of [N-methyl 34Q]-PYY₃₋₃₅ as the major metabolite of [N-methyl 34Q]-PYY₃₋₃₆ in mini-pig (50 nmol/kg, i.v., n=2) The MS spectrum is from LC-MS analysis of a pool of two plasma samples taken 30 min after dosing. The monoisotopic masses can be seen in Table 5.

Table 1 Metabolism of PYY₃₋₃₆ in Göttingen mini-pig and Rhesus monkey (50 nmol/kg, i.v., 10 min). The area under the curve (AUC) was calculated from LC-MS responses from the time profiles shown in Figure 4. The most intense charge state is indicated in bold. ND, not detected. All m/z values were determined with a mass accuracy below 2 ppm.

Parent (or metabolite)	Monoisotopic m/z observed (z)	% of AUC _{parent}	
		Mini-pig	Rhesus Monkey
PYY ₃₋₃₆	579.1607 (7), 675.5201 (6) , 810.4223 (5), 1012.7764 (4)	100%	100%
PYY ₃₋₃₅	648.5049 (6)	2%	5%
PYY ₃₋₃₄	622.4890 (6), 746.7859 (5) , 933.2305 (4)	33%	23%
PYY ₃₋₃₃	601.1462 (6), 721.1740 (5)	<1%	<1%
PYY ₃₋₃₂	689.9541 (5)	<1%	ND
PYY ₃₋₃₀	649.9306 (5) , 812.1615 (4)	4%	4%
PYY _{3-29/4-30}	627.3143 (5) , 783.8915 (4)	1%	ND
PYY _{3-27/4-28}	581.8886 (5) , 727.1086 (4)	ND	<1%
PYY ₃₋₂₆	549.2755 (5) , 686.3416 (4)	ND	<1%
PYY ₆₋₃₆	619.1468 (6), 742.7750 (5)	1%	2%

Table 2 Metabolism of PYY₁₋₃₆ in mini-pig (50 nmol/kg, i.v., n=2). The area under the curve (AUC) was based on LC-MS responses from the time profiles (supplementary data, Figure S2). The most intense charge state is indicated in bold. All m/z values were determined with a mass accuracy below 4 ppm.

Parent (or metabolite)	Monoisotopic m/z observed (z)	% of AUC _{parent}
PYY ₁₋₃₆	616.3224 (7), 718.8738 (6) , 862.4476 (5)	100%
PYY ₁₋₃₄	665.8441 (6), 798.8112 (5)	7%
PYY ₂₋₃₆	593.0265 (7), 691.6963 (6)	29%
PYY ₂₋₃₄	638.6659 (6), 766.1986 (5)	5%
PYY ₃₋₃₆	579.1616 (7), 675.5211 (6) , 810.4237 (5), 1012.7777 (4)	55%
PYY ₃₋₃₄	622.4910 (6), 746.7874 (5) , 933.2323 (4)	27%
PYY ₃₋₃₀	649.9331 (5), 812.1628 (4)	< 1%

Table 3 Metabolism of PYY₃₋₃₅ in a mini-pig (50 nmol/kg, *i.v.*). The area under the curve (AUC) was based on LC-MS responses from the time profiles shown in Figure 5. The most intense charge state is indicated in bold. All m/z values were determined with a mass accuracy below 2 ppm.

Parent (or metabolite)	Monoisotopic m/z observed (z)	% of AUC _{parent}
PYY ₃₋₃₅	556.0053 (7), 648.5050 (6) , 778.0047 (5), 972.2542 (4)	100%
PYY ₃₋₃₄	622.4890 (6), 746.7861 (5) , 933.2294 (4), 1243.9690 (3)	1094%
PYY ₃₋₃₀	649.9293 (5) , 812.1601 (4)	74%
PYY _{3-29/4-30}	627.3125 (5) , 783.8884 (4)	12%
PYY _{3-27/4-28}	581.8870 (5) , 727.1071 (4)	13%
PYY ₃₋₂₆	549.2746 (5) , 686.3415 (4)	8%

Table 4 Metabolism of PYY₃₋₃₄ in mini-pig (50 nmol/kg, i.v., n=2). The area under the curve (AUC) was based on LC-MS responses from the time profiles. The most intense charge state is indicated in bold. All m/z values were determined with a mass accuracy below 3 ppm.

Parent (or metabolite)	Monoisotopic m/z observed (z)	% of AUC _{parent}
PYY ₃₋₃₄	622.4891 (6), 746.7861 (5) , 933.2303 (4), 1243.972 (3)	100%
PYY ₃₋₃₀	649.9296 (5) , 812.1606 (4)	6%
PYY _{3-29/4-30}	627.3132 (5) , 783.8894 (4)	1%
PYY _{3-27/4-28}	581.8875 (5) , 727.1061 (4)	1%
PYY ₃₋₂₆	549.2755 (5)	<1%
PYY ₆₋₃₄	679.1392 (5)	<1%

Table 5 Metabolism of [*N*-methyl Q34]-PYY₃₋₃₆ in mini-pig (50nmol/kg, *i.v.*, n=2). The area under the curve (AUC) was based on LC-MS responses from the time profiles. In bold, the most intense charge state is indicated. All m/z values were determined with a mass accuracy below 2 ppm.

Parent (or metabolite)	Monoisotopic m/z observed (z)	% of AUC _{parent}
PYY ₃₋₃₆	581.1632 (7), 677.8564 (6) , 813.2259 (5), 1016.2804 (4), 1354.7052 (3)	100%
PYY ₃₋₃₅	558.0085 (7), 650.8429 (6) , 780.8100 (5), 975.7596 (4)	53%
PYY ₃₋₃₀	649.9309 (5) , 812.1618 (4), 1082.5461 (3)	3%
PYY _{3-27/4-28}	581.8889 (5) , 727.1089 (4)	<1%
PYY ₆₋₃₆	745.5781 (5)	1%

Supplementary Data

Figure S1 LC-MS analysis of a 200 nM plasma standard of A. PYY₃₋₃₆, B. PYY₃₋₃₅, C. PYY₃₋₃₄ and D. PYY₁₋₃₆.

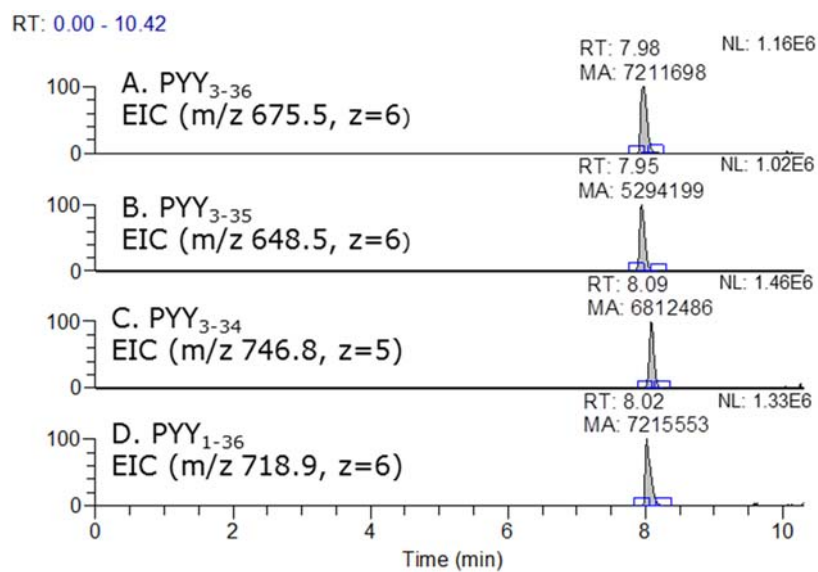


Table S1 Metabolism of PYY₃₋₃₆ in Rhesus monkey (n=3, 50 nmol/kg, i.v.). The area under the curve (AUC) was based on LC-MS responses from time profiles. In bold, the most intense charge state is indicated. All m/z values were determined with a mass accuracy below 3 ppm.

Parent (or metabolite)	Monoisotopic m/z observed (z)	% of AUC _{parent}
PYY ₃₋₃₆	579.1612 (7), 675.5206 (6) , 810.4228 (5), 1012.7758 (4)	100%
PYY ₃₋₃₅	648.5070 (6)	5%
PYY ₃₋₃₄	622.4897 (6), 746.7864 (5) , 933.2271 (4)	23%
PYY ₃₋₃₃	721.1742 (5)	<1%
PYY ₃₋₃₀	649.9312 (5) , 812.1612 (4)	4%
PYY _{3-27/4-28}	581.8886 (5) , 727.1086 (4)	<1%
PYY ₃₋₂₆	549.2755 (5) , 686.3416 (4)	<1%
PYY ₆₋₃₆	742.7755 (5)	2%

Figure S2 Time profile of PYY₁₋₃₆ and the three most abundant metabolites after dosing to mini-pigs (i.v., 50 nmol/kg, n=2). The LC-MS response came from peak integration of extracted ion chromatograms.

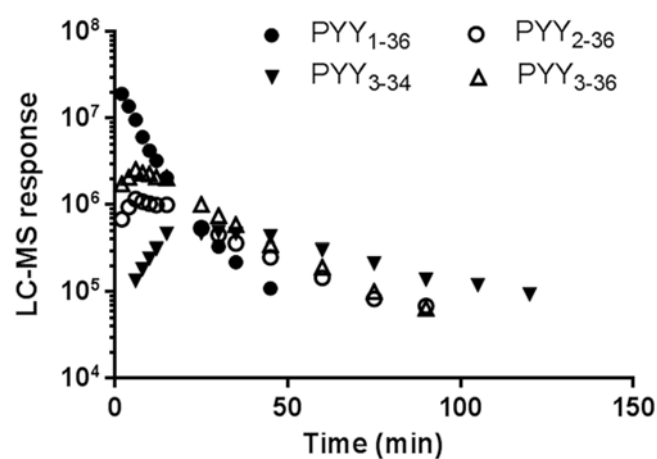


Figure S3 Plasma stability of PYY₃₋₃₆ and PYY₃₋₃₅ in heparin stabilised plasma from minipig.

Experiments were conducted with and without 10 mM EDTA. Data are shown as mean \pm SD (n=4). A) Stability of PYY₃₋₃₆. B) Metabolite formation following incubation of PYY₃₋₃₆ with plasma for 120 min. C) Stability of PYY₃₋₃₅. D) Metabolite formation following incubation of PYY₃₋₃₅ with plasma for 15 min.

